



HHS Public Access

Author manuscript

Nucl Med Biol. Author manuscript; available in PMC 2016 December 01.

Published in final edited form as:

Nucl Med Biol. 2015 December ; 42(12): 967–974. doi:10.1016/j.nucmedbio.2015.07.006.

[carbonyl-¹¹C]4-Fluoro-*N*-methyl-*N*-(4-(6-(methylamino)pyrimidin-4-yl)thiazol-2-yl)benzamide ([¹¹C]FIMX) is an effective radioligand for PET imaging of metabotropic glutamate receptor 1 (mGluR1) in monkey brain

Jinsoo Hong, Shuiyu Lu, Rong Xu, Jeih-San Liow, Alicia E. Woock, Kimberly J. Jenko, Robert L. Gladding, Sami S. Zoghbi, Robert B. Innis, and Victor W. Pike*

Molecular Imaging Branch, National Institute of Mental Health, National Institutes of Health, Building 10, Room B3 C346A, 10 Center Drive, Bethesda, Maryland 20892-1003, United States

Abstract

Introduction—Metabotropic glutamate subtype receptor 1 (mGluR1) is implicated in several neuropsychiatric disorders and is a target for drug development. [¹⁸F]FIMX ([¹⁸F]4-fluoro-*N*-methyl-*N*-(4-(6-(methylamino)pyrimidin-4-yl)thiazol-2-yl)benzamide) is an effective radioligand for imaging brain mGluR1 with PET. A similarly effective radioligand with a shorter half-life would usefully allow PET studies of mGluR1 at baseline and after pharmacological or other challenge on the same day. Here we describe the preparation of [¹¹C]FIMX for evaluation in monkey with PET.

Methods—[¹¹C]FIMX was prepared via Pd-promoted carbonylation of 1-fluoro-4-iodobenzene with [¹¹C]carbon monoxide, aminolysis of the [¹¹C]acyl-palladium complex with the requisite Boc-protected amine, and deprotection with HCl in THF. PET scans of [¹¹C]FIMX injected into a monkey were performed at baseline and after preblock of mGluR1 with measurement of the arterial input function.

Results—The radiosynthesis required 42 min and gave [¹¹C]FIMX in about 5% overall decay-corrected radiochemical yield and with a specific activity of about 100 GBq/μmol. PET in rhesus monkey at baseline showed that radioactivity peaked high in receptor-rich cerebellum and much lower in receptor-poor occipital cortex. Radioactivity in cerebellum declined to 32% of peak at 85 min. V_T at baseline appeared stable in all brain regions after 60 min. Under mGluR1 pre-blocked condition, radioactivity uptake in all regions declined more rapidly to a low level. Receptor pre-block reduced V_T from 13.0 to 1.5 in cerebellum and from 2.9 to 1.4 in occipital cortex.

Conclusion—[¹¹C]FIMX is an effective radioligand for imaging mGluR1 in monkey with PET.

Corresponding author: Dr. Victor W. Pike, Molecular Imaging Branch, National Institute of Mental Health, National Institutes of Health, Building 10, Room B3 C346A, 10 Center Drive, Bethesda, Maryland 20892-1003, United States, Tel: 301 594 5986, Fax: 301 480 5112, pikev@mail.nih.gov.

Publisher's Disclaimer: This is a PDF file of an unedited manuscript that has been accepted for publication. As a service to our customers we are providing this early version of the manuscript. The manuscript will undergo copyediting, typesetting, and review of the resulting proof before it is published in its final citable form. Please note that during the production process errors may be discovered which could affect the content, and all legal disclaimers that apply to the journal pertain.

Keywords

mGluR1; radioligand; PET; carbon-11; monkey; brain

1 Introduction

Glutamate is the major excitatory neurotransmitter in brain and acts on a multitude of receptor types, including two major classes of ionotropic (iGluR) and metabotropic (mGluR) receptors. The former are ligand-gated ion channels whereas the latter are G-protein-coupled receptors. The metabotropic receptors are further classified into three main groups. Receptors 1 (mGluR1) and 5 (mGluR5) constitute Group 1, and they are closely related structurally and functionally [1,2]. Their distributions in brain are however very distinct, with mGluR5 most highly represented in cerebrum [3] and mGluR1 in cerebellum [4,5]. mGluR5 and mGluR1 are implicated in several neuropsychiatric disorders [2,6], notably autism (Fragile X), anxiety and psychosis for mGluR5, and anxiety, mood disorders, stroke, epilepsy, pain, and schizophrenia for mGluR1 [7]. These receptors are also prominent targets for experimental drugs [8–13].

Radioligands for quantifying brain receptors with PET have value for neuropsychiatric research and also for drug development. PET radioligands for quantifying mGluR5 in human brain have reached an advanced stage of development and application [14–16]. PET radioligand development for mGluR1 has also been strenuously pursued [17–22]. Hostetler et al. [18] showed that [¹⁸F]MK-1312 ([¹⁸F]5-(1-(2-fluoropyridin-3-yl)-5-methyl-1*H*-1,2,3-triazol-4-yl)-2-propylisoindolin-1-one; Chart 1) could be applied to measure monkey brain mGluR1 receptor occupancy by an experimental drug (MK-5435). Yamasaki et al. [23] reported on the promising performance of two structurally-related candidate PET radioligands in rhesus monkey, namely [¹¹C]ITMM ([¹¹C]*N*-[4-[6-(isopropylamino)pyrimidin-4-yl]-1,3-thiazol-2-yl]-4-methoxy-*N*-methylbenzamide; Chart 1) and [¹¹C]ITDM ([¹¹C]*N*-[4-[6-(isopropylamino)pyrimidin-4-yl]-1,3-thiazol-2-yl]-4-methyl-*N*-methylbenzamide; Chart 1). Only two PET radioligands have thus far reached evaluation in human subjects [24,25]. Thus, [¹¹C]ITMM showed moderate brain uptake in humans and slow kinetics, which impair attempts at robust quantification [24]. By contrast, we have found that the much higher-affinity ($IC_{50} = 1.8$ nM) mGluR1 radioligand [¹⁸F]FIMX ([¹⁸F]4-fluoro-*N*-methyl-*N*-(4-(6-(methylamino)pyrimidin-4-yl)thiazol-2-yl)benzamide; Chart 1) has excellent PET imaging characteristics for mGluR1 quantification both in monkey [21] and in human [25], including high brain uptake, high receptor-specific signal and quantifiable reversible kinetics.

The 110-min half-life of fluorine-18 does pose a limitation on the number of times that [¹⁸F]FIMX may be injected into the same animal or human subject on the same day. For some studies, it may be desirable to inject a radioligand more than once into the same subject on one day, such as in receptor occupancy studies aiming to assess the effect of pharmacological challenges on receptor availability [17,26]. Such studies become feasible with a shorter-lived carbon-11 ($t_{1/2} = 20.4$ min) label. Therefore, we sought to synthesize [¹¹C]FIMX to provide an effective shorter-lived mGluR1 PET radioligand.

Our studies with [¹⁸F]FIMX have shown that [¹⁸F]4-fluorobenzoic acid is a major radiometabolite arising from amide bond hydrolysis in periphery [25]. Although each methyl group in FIMX is an appealing site for labeling with carbon-11, we considered that labeling at either of these positions would risk generating the amine [¹¹C]**3** (Scheme 1) and also possibly derivatives as potentially brain-penetrant radiometabolites that might confound robust quantification of radioligand binding to mGluR1 [27]. Therefore, to circumvent this possible problem, we set out to label FIMX in the carbonyl group.

2 Results and Discussion

2.1 Chemistry and radiochemistry

[¹¹C]Carbon monoxide is readily prepared on-line from cyclotron-produced [¹¹C]carbon dioxide [28] and has immense utility for labeling organic molecules in carbonyl positions [29], including carbonyl groups in aryl carboxamides through transition-metal mediated carbonyl insertion reactions between aryl halides and secondary amines [30–33]. Such reactions generally tolerate wide functionality and may be conducted rapidly to give high radiochemical yields. Different practical procedures have been reported. A single-pot procedure consists of heating the [¹¹C]carbon monoxide, Pd reagent, iodoarene, and amine together in an autoclave. Another procedure treats iodoarene with Pd reagent and [¹¹C]carbon monoxide to form the [¹¹C]acyl-Pd complex, before treating this complex with amine in a second vessel. Recently, Andersen et al. [33] demonstrated that aryl-Pd complexes could be pre-formed, purified and stored before being used in a modified one-pot procedure to synthesize [¹¹C]amides, even for some structurally demanding labeling targets. Here we aimed to implement the conventional two-stage two-pot procedure. No comparison of methods or detailed optimizations were performed, as the main objective was to obtain [¹¹C]FIMX in adequate activity (~ 400 MBq) for evaluation of performance in monkey.

We synthesized **3** (Scheme 1) to act as the secondary amine partner in a [¹¹C]carbonyl insertion reaction with 4-fluoro-1-iodobenzene. This precursor carries a Boc protecting group at the pyrimidinyl *N*-methyl group so that only the secondary *N*-methylamino group on the thiazole ring may be involved in the coupling reaction. The reported synthesis of [¹⁸F]FIMX [21] uses a similarly protected precursor, showing that this protecting group may be removed within minutes. Precursor **3** was obtained in moderate overall yield in three steps from commercially available **1**.

A greatly modified [34] Synthia-type [35] radiosynthesis platform, incorporating a module for generating [¹¹C]carbon monoxide and a micro-autoclave [36], was used for automated radiochemistry. Although a wide range of palladium reagents is available for carbonyl insertion reactions, only Pd(Ph₃)₄ was used in this study (Scheme 2). Pd(Ph₃)₄ is slightly air and light sensitive. We observed that [¹¹C]carbon monoxide insertion efficiency decreased over several syntheses conducted with the same source and weight of reagent, despite storage of the reagent in a nitrogen-protected glove-box, with only occasional removal within 1 h before any use. [¹¹C]Carbon monoxide insertion efficiency could be restored by increasing the weight of Pd(Ph₃)₄ used from the same batch by 20 to 30%. THF was preferred as solvent because of its easy removal before the aminolysis. The THF had to be fresh and anhydrous to achieve optimal insertion and minimal formation of [¹¹C]4-

fluorobenzoic acid. The other reagents could be handled in open air. One aspect of the procedure for the aminolysis was important. If the [^{11}C]acyl-Pd complex in THF was first transferred to a 5-mL glass vial at elevated temperature (110 °C), and then a THF solution of **3** was added, the [^{11}C]acyl-Pd complex was vulnerable to reaction with trace moisture to form [^{11}C]4-fluorobenzoic acid and was no longer able to form Boc-protected [^{11}C]FIMX. If a solution of **3** and tributylamine in THF was preloaded into the 5-mL glass vial and the [^{11}C]acyl-Pd complex solution then transferred at a lower temperature (< 80 °C), the aminolysis reaction went smoothly upon the complete evaporation of THF. Finally, the Boc-protecting group was readily removed with 1.1 M HCl in THF (550 μL) with heating for 1 min at about 100 °C. [^{11}C]FIMX was readily separated from the reaction mixture by reversed phase HPLC and formulated as a sterile solution for intravenous injection.

Radiochemically pure ($99.3 \pm 0.9\%$) doses of [^{11}C]FIMX were obtained with activities of 933 ± 396 MBq and specific activities of 102 ± 31 GBq/ μmol at 42 ± 3 min ($n = 4$) from the end of radionuclide production. Product identity was confirmed by observation of comobility with authentic FIMX on radio-HPLC and also by LC-MS of carrier ($[\text{M}+\text{H}]^+$, observed: 344.1; calculated: 344.09). HPLC showed that [^{11}C]FIMX formulated in saline containing ethanol (10% v/v) was > 97% unchanged after 1 h at room temperature.

2.2 Lipophilicity (logD) measurement

Lipophilicity influences several PET radioligand imaging characteristics, including plasma free fraction (f_p), brain penetration, non-specific binding and susceptibility to metabolism [37–40]. Knowledge of logD, as an index of lipophilicity, is useful, for example, for benchmarking the lipophilicities of radiometabolites. The logD of [^{11}C]FIMX was determined essentially by a previously described technique [41] based on distribution of the radioligand between 1-octanol and sodium phosphate buffer (0.15 M; pH 7.4), but with a correction for radioligand instability because it was found that [^{11}C]FIMX degraded in the buffer to $79.1 \pm 3.3\%$ ($n = 4$) of its original radiochemical purity over 57 min at room temperature (Fig. 1). With appropriate correction for this instability, the logD of [^{11}C]FIMX was found to be 3.27 ± 0.03 ($n = 6$), and appreciably higher than the value (2.52) [21] that had been obtained without this correction.

2.3 PET imaging of monkey brain

Intravenous administration of [^{11}C]FIMX into a rhesus monkey at baseline resulted in high brain radioactivity uptake (Fig. 2; left panel). Regional radioactivity uptakes reflected known mGluR1 density and peaked at around 12.5 min. Peak uptakes were highest in receptor-rich cerebellum (8.50 SUV), moderate in thalamus (6.00 SUV), hippocampus (4.47 SUV), frontal cortex (4.23 SUV), and occipital cortex (3.67 SUV), and lowest in the rest of the brain. Peak radioactivity uptakes in all regions were followed by a smooth decrease in radioactivity level, for example, in receptor-rich cerebellum by 32% to 5.74 SUV at 85 min after injection. This rate of decrease was close to that previously reported for [^{18}F]FIMX (37% at 90 min after injection) [21]. Summed PET images (Fig. 3, upper row) reflected the expected distribution of mGluR1 receptors, as previously seen with [^{18}F]FIMX [21].

In the receptor preblocked experiment, the same monkey was administered intravenously with a selective mGluR1 antagonist (3,4-dihydro-2*H*-pyrano[2,3-*b*]quinolin-7-yl)-(cis-4-methoxycyclohexyl)-methanone, JNJ-16259685; 3 mg/kg) [42] at 5 min before the injection of [¹¹C]FIMX. In this experiment, all regional time-activity curves were almost indistinguishable, showing a fast smooth decline from a marginally higher peak radioactivity level (Fig. 2, right panel). Summed images showed that the distribution of radioactivity across brain became low and uniform (Fig. 3, lower row), so indicating that a high level of brain radioactivity in the baseline experiment was due to specific binding to mGluR1.

2.4 Plasma free fraction (f_p)

Only radioligand that is free in plasma is considered to be able to penetrate the blood-brain barrier. The plasma-free fraction (f_p) of [¹¹P C]FIMX for rhesus monkey was found to be 0.016 ± 0.001 ($n = 3$) at baseline. This value is similar to that previously measured with [¹⁸F]FIMX [21]. The f_p value increased to 0.042 ± 0.003 ($n = 3$) under the pre-blocked condition. These f_p values are in the range expected for a radioligand with a measured logD value of 3.27 [41].

2.5 Stability of [¹¹C]FIMX in monkey brain homogenates

[¹¹C]FIMX was found to be 99.4% unchanged when incubated with monkey brain homogenates for 30 min at room temperature.

2.6 Stability of [¹¹C]FIMX in monkey whole blood and plasma

When [¹¹C]FIMX was incubated for 30 min at room temperature with monkey whole blood or plasma from the baseline and preblock PET experiments, [¹¹C]FIMX was 92% and 91% unchanged, respectively.

2.7 Emergence of radiometabolites in monkey plasma

After intravenous injection of [¹¹C]FIMX into monkey, radioactivity decreased rapidly in plasma. HPLC analysis of arterial plasma during the scanning period, showed that the percentage of radioactivity in plasma represented by [¹¹C]FIMX was lower at baseline than under the preblocked condition up to about 1 h (Fig. 4). [¹¹C]FIMX represented 31 and 21% of total radioactivity at 10 and 30 min, respectively, at baseline. The corresponding values under the preblocked condition were 43 and 31%, respectively. After 1 h from intravenous radioligand injection, the percentage of radioactivity represented by [¹¹C]FIMX changed very little at baseline but continued to fall slowly in the pre-blocked experiment.

Four radiometabolites ([¹¹C]A–[¹¹C]D) were detected in plasma at 30 min after radioligand injection, and these were all less lipophilic than [¹¹C]FIMX, as judged by their shorter retention times in reversed-phase HPLC (Fig. 5). One radiometabolite ([¹¹C]B) was identified as [¹¹C]4-fluorobenzoic acid. The other radiometabolites were not identified. Their lower lipophilicities relative to [¹¹C]FIMX (logD, 3.27) may restrict their brain entry to contaminate receptor-specific signal. Continuous declines in the time-activity curves for monkey brain regions following intravenous injection of [¹¹C]FIMX throughout the scanning period (Fig. 2) suggest that entry of radiometabolites into brain was indeed limited.

2.8 Two-tissue compartmental modeling of PET data

Two-tissue compartmental modeling (Fig. 6) showed that the total volume of distribution (V_T) in receptor-rich cerebellum decreased from 13.0 to 1.5, a reduction close to 90%. V_T in receptor-poor occipital cortex decreased from 2.9 to 1.4. After preblock, V_T in all regions decreased to 1.4. For baseline scans, the two-tissue compartment model showed that V_T values are within 10% of the terminal value by 40 min of imaging (Fig. 7). [^{11}C]FIMX binding to receptors in the brain can be quantified from about 60 min of PET imaging data along with the measured plasma arterial input function. The stable V_T values again indicate a lack of accumulation of radiometabolites in the brain, consistent with the observations that all radiometabolites in plasma were less lipophilic than [^{11}C]FIMX (Fig. 5) and that [^{11}C]FIMX was not metabolized by monkey brain homogenates in vitro.

2.9 Comparison of [^{11}C]FIMX with other prominent ^{11}C -labeled mGluR1 radioligands

Hitherto, the most promising ^{11}C -labeled radioligands for imaging mGluR1 in monkey brain, appear to have been [^{11}C]ITMM and [^{11}C]ITDM (Chart 1) [23]. However, each of these radioligands has much lower peak uptake in mGluR1-rich rhesus monkey cerebellum (< 1.3 SUV), and much lower V_T (≈ 3.6 mL/cm 3) than the much higher-affinity [^{11}C]FIMX (8.5 SUV and 13 mL/cm 3 respectively). Moreover, the relative proportion of V_T represented by specific binding (V_S) has not been estimated through receptor blocking experiments for [^{11}C]ITMM and [^{11}C]ITDM, whereas a very high proportion of the signal obtained in rhesus monkey cerebellum with [^{11}C]FIMX appears to be specific binding. [^{11}C]FIMX is clearly superior to [^{11}C]ITMM or [^{11}C]ITDM for monkey mGluR1 imaging, likely due in large measure to its higher affinity.

3 Experimental

3.1 General methods

All chemicals were purchased from commercial sources and used as received.

^1H - (400.13 MHz) and ^{13}C - (100.62 MHz) NMR spectra were recorded at room temperature on an Avance-400 spectrometer (Bruker; Billerica, MA). Chemical shifts are reported in δ units (ppm) downfield relative to the chemical shift for TMS. Abbreviations s, d, t, and q denote singlet, doublet, triplet, and quartet, respectively. HRMS data were acquired at the Mass Spectrometry Laboratory, University of Illinois at Urbana-Champaign (Urbana-Champaign, IL) under electron ionization conditions using a double-focusing high-resolution mass spectrometer (Micromass, Waters; Milford, MA). Synthesized compounds were analyzed with LC-MS on an LCQ Deca instrument (Thermo Fisher Scientific Corp.; Waltham, MA).

γ -Radioactivity from ^{11}C was measured with a calibrated dose calibrator (Atomlab 300; Biodex Medical Systems; Shirley, NY) or a γ -counter (Wallac Wizard 3", 1480 automatic γ -counter; PerkinElmer; Waltham, MA). Radioactivity measurements were corrected for physical decay. All radiochemistry was performed in a lead-shielded hot-cell for radiation safety to personnel. Decay-corrected radiochemical yields are estimated for formulated [^{11}C]FIMX from the estimated initial amount of [^{11}C]carbon dioxide.

3.2 Synthesis

***tert*-Butyl 6-(1-ethoxyvinyl)pyrimidin-4-yl(methyl)carbamate (2).** Pd(PPh₃)₄ (0.49 g, 0.42 mmol), CsF (4.2 g, 28 mmol) and CuI (0.27 g, 1.4 mmol) were added to a solution of *tert*-butyl 6-chloropyrimidin-4-yl(methyl)carbamate (**1**; 3.3 g, 14 mmol) and *tri*-butyl(1-ethoxyvinyl)stannane (5.0 g, 14 mmol) in DMF (60 mL). The solution was degassed with a stream of argon for 20 min then heated at 80 °C for 5.5 h under argon. The solution was then cooled to room temperature, quenched with CH₂Cl₂/H₂O (1: 1 v/v), and filtered through Celite. The aqueous layer was extracted three times with CH₂Cl₂. The organic layers were combined and dried over MgSO₄. Solvent was removed with a rotary evaporator. Silica gel chromatography (EtOAc: hexane; 1: 20 v/v) of the residue gave **2** as a white solid (2.5 g, 66%). ¹H-NMR (CDCl₃): δ 1.44 (3H, t), 1.58 (9H, s), 3.45 (3H, s), 3.97 (2H, q), 4.48 (1H, d, *J* = 2 Hz), 5.57 (1H, s), 8.14 (1H, d, *J* = 1.2 Hz), 8.85 (1H, s, *J* = 1.2 Hz). ¹³C-NMR (CDCl₃): δ 14.48, 28.23, 33.29, 63.67, 82.63, 87.53, 108.15, 153.55, 156.90, 157.11, 160.10, 161.89. LC-MS: *m/z* [M + H]⁺, 280.2; HRMS: calc'd for C₁₄H₂₂N₃O₃ [M + H]⁺, 280.1661; found, 280.1653.

***tert*-Butyl methyl(6-(2-(methylamino)thiazol-4-yl)pyrimidin-4-yl)carbamate (3).** A solution of **2** (1.0 g, 3.60 mmol) and *N*-bromo-succinimide (NBS) (0.7 g, 4.0 mmol) in a mixture of THF (20 mL) and H₂O (20 mL) was stirred at room temperature for 2 h. 1-Methyl thiourea (0.32 g, 1.79 mmol) was added and the reaction mixture stirred for 2 h. Solvent was then evaporated off. Silica gel chromatography (CH₂Cl₂: MeOH; 20: 1 v/v) of the residue gave **3** as a light brownish foam (1.08 g, 94%). ¹H-NMR (CDCl₃): δ 1.57 (9H, s), 2.99 (3H, d), 3.47 (3H, s), 5.30 (1H, s), 7.32 (1H, s), 8.47 (1H, s), 8.87 (1H, s). ¹³C NMR (CDCl₃): δ 28.18, 32.10, 33.17, 82.48, 108.56, 109.17, 149.86, 153.55, 157.37, 158.93, 161.70, 170.89. LC-MS: *m/z* [M + H]⁺, 322.2; HRMS: calc'd for C₁₄H₂₀N₅O₂S [M + H]⁺, 322.1338; found, 322.1331.

3.3 Radiosynthesis

[¹¹C]Carbon dioxide was produced via the ¹⁴N(p,α)¹¹C reaction in a target containing 1% oxygen in nitrogen, initially pressurized to 225 psi. This target was bombarded with a beam (45 μA) of protons (16.5 MeV) from a PETtrace cyclotron (GE Medical Systems; Milwaukee, WI). At the end of irradiation, radioactivity was released to a trap containing molecular sieve (13X; 300 mg) at room temperature, which was then swept with helium at 80 mL/min to remove residual oxygen. Irradiations were conducted for 40 min for radiotracer production and typically provided about 110 GBq of trapped [¹¹C]carbon dioxide. Shorter irradiations were used to produce lower amounts of [¹¹C]carbon dioxide for radiochemistry experiments.

[¹¹C]Carbon dioxide was released from the molecular sieve trap at 280 °C in a stream of helium (10 mL/min) for concentration in another trap containing silica (10 mg) cooled in liquid nitrogen. This trap was heated with a halogen lamp (150 W) to release [¹¹C]carbon dioxide into helium (10 mL/min) for conversion into [¹¹C]carbon monoxide by passage over a heated (875 °C) quartz tube (22 cm length; 0.7 cm i.d.) packed with molybdenum wire (99.97%, 0.05 mm diameter; Strem Chemicals, Newburyport, MA). The effluent was passed through ascarite to trap unconverted [¹¹C]carbon dioxide and the [¹¹C]carbon monoxide was

then trapped in a second silica trap at $-196\text{ }^{\circ}\text{C}$. By heating this trap with a halogen lamp, $[^{11}\text{C}]$ carbon monoxide was released in helium for transfer to an autoclave [36] containing $\text{Pd}(\text{Ph}_3)_4$ (2.6 μmol) and 4-fluoro-1-iodobenzene (14 μmol) in THF (80 μL). The autoclave was then pressurized to 3500 psi with THF from a HPLC pump (SSI Isocratic; Scantech Lab, Sweden) and heated to $130\text{ }^{\circ}\text{C}$ for 4 min. The reaction mixture was then flushed out of the autoclave into a 5-mL Alltech glass vial (Sigma Aldrich; St Louis, MI) that had been loaded with a solution of the Boc-protected precursor **3** (2.2 μmol) and Bu_3N (9.1 μmol) in THF (200 μL). The vial was heated from 80 to $110\text{ }^{\circ}\text{C}$ while THF was evaporated off to dryness through a vent needle over about 6.5 min. Then a solution of HCl in THF (1.1 M; 550 μL) was added, and the mixture further heated for 1 min at about $100\text{ }^{\circ}\text{C}$. Finally water (2.5 mL) was added to quench the reaction. The aqueous mixture was injected onto a Luna C18 column (10 μm , $10 \times 250\text{ mm}$; Phenomenex; Torrance, CA) eluted at 6 mL/min, initially with (MeCN: 0.1% formic acid (25: 75 v/v) for 1 min, and then with the MeCN component increased linearly to 70% over 10 min, and to 90% at 11 min. Absorbance was monitored at 254 nm (System Gold 166; Beckman Coulter Inc., Pasadena, CA) while radioactivity was monitored with a pin-diode detector (Bioscan Inc., Washington DC). The fraction eluting between 6.9 and 7.5 min was collected and concentrated under vacuum at $80\text{ }^{\circ}\text{C}$ for 1 min. The radioactive residue was reconstituted in 10% ethanol in saline (10 mL), and sterilized by filtration through a 0.22 μm sterile filter (Millipore-MP; Waters Corp.; Milford, MA).

An aliquot (100 μL) of the formulated product was analyzed with radio-HPLC on a Gemini-NX column (5 μm , $4.6 \times 250\text{ mm}$; Phenomenex) to obtain radiochemical purity, chemical purity and specific activity. The column was eluted at 2 mL/min with MeCN: 0.1% TEA in water (45: 55 v/v) with eluate monitored for absorbance at 254 nm (System Gold 166 detector) and for radioactivity with a PMT detector (Bioscan Inc.). Retention time of $[^{11}\text{C}]$ FIMX was 3.9 min. The absorbance response had been pre-calibrated with respect to mass of FIMX in the injectate, to permit calculation of specific activity.

3.4 Lipophilicity measurements and stability in aqueous buffer

The value for the distribution coefficient ($\log D$) of $[^{11}\text{C}]$ FIMX between 1-octanol and sodium phosphate buffer (0.15 M, pH 7.4) was determined essentially with a technique described previously [41], but with correction for radioligand instability in the buffer phase. For the purpose of measuring the degree of instability, formulated $[^{11}\text{C}]$ FIMX solution was placed in sodium phosphate buffer (0.15 M; pH 7.4) for the duration of a $\log D$ determination, and reanalyzed by radio-HPLC on an X-Terra C18 column (10 μm ; $7.8 \times 300\text{ mm}$; Waters Corp.) eluted with MeOH: H_2O : Et_3N (65: 35: 0.1 by vol.) at 4.5 mL/min. For the $\log D$ determination, the percentage of radioactivity represented by unchanged $[^{11}\text{C}]$ FIMX in the aqueous buffer at the end of extraction with 1-octanol was determined with radio-HPLC.

3.5 Stability of $[^{11}\text{C}]$ FIMX in monkey brain homogenate

Monkey brain tissue, that had been stored at $-70\text{ }^{\circ}\text{C}$, was thawed on the day of the experiment. Formulated $[^{11}\text{C}]$ FIMX solution (2.8 MBq; 11 μL) was incubated with monkey brain homogenate (0.06 g; 500 μL) in phosphate-buffered saline (pH 7.4) for 30 min at room

temperature, and then analyzed by reversed phase HPLC to measure change in radiochemical purity.

3.6 Analysis of radiometabolites in monkey blood and plasma

Experiments were performed to verify the stability of [^{11}C]FIMX in whole monkey blood and plasma to ensure that no significant degradation of [^{11}C]FIMX would occur between blood sampling from monkey and processing for the analysis of radiometabolites. Thus, formulated [^{11}C]FIMX solution ($\sim 23 \mu\text{L}$; $< 35 \text{ kBq}$) was incubated with monkey whole blood (200 μL) and monkey plasma (200 μL) at room temperature for at least 30 min. After incubation, the radioactive whole blood sample (200) was mixed with distilled water (300 μL) for 30 s to lyse blood cells. Samples of the lysed cells (450 μL) and of the incubated radioactive plasma were each added to MeCN (720 μL) for deproteinization. The samples were then centrifuged (10,000 g) and the clear supernatant liquids were analyzed with radio-HPLC. The precipitates were counted in a γ -counter to allow calculation of the extraction efficiency. The extraction efficiency of all samples was high at $91.5 \pm 7.4\%$ ($n = 6$). The percentage of unchanged radioligand in the analyte, as determined by radio-HPLC, was divided by the radiochemical purity of the radioligand to give the stabilities of the radioligand in whole blood and plasma.

For the analysis of [^{11}C]FIMX and radiometabolites in plasma, arterial blood samples were collected at different times after intravenous injection of [^{11}C]FIMX into a male rhesus monkey (13.2 kg). Plasma was separated and analyzed with radio-HPLC on a Novapak C18 column (4 μm , $100 \times 8 \text{ mm}$; Waters Corp.; Milford, MA) housed in a radial compression module (RCM-100) and eluted at 2.0 mL/min with MeOH: H_2O : Et_3N (65: 35: 0.1 by vol.), as described previously.[42] Full recoveries of radioactivity from these HPLC analyses were routinely verified. Radioactivity levels in different blood components were expressed as standardized uptake value (SUV), defined as $[(\% \text{ injected activity}/\text{cm}^3) \times \text{body weight (g)}]/100$.

3.7 Plasma free fraction determination

Plasma-free fractions for [^{11}C]FIMX in monkey plasma were determined by a method described previously [44].

3.8 PET Imaging

PET imaging experiments in monkey were performed in accordance with the Guide for Care and Use of Laboratory Animals [45] and were approved by the National Institute of Mental Health Animal Care and Use Committee.

PET Scans—A single rhesus monkey (*Macaca mulatta*; 13.2 kg), anesthetized with ketamine (10 mg/kg, i.m.) and then maintained in anesthesia with 1.6% isoflurane and 98.4% O_2 , was used for two PET scan sessions. Thus, at baseline, [^{11}C]FIMX (192 MBq; 39.8 GBq/ μmol) was injected intravenously as a bolus. Under receptor-preblocked condition at more than 3 h later on the same day, JNJ16259685, a selective mGluR1 ligand (3 mg/kg), was administered intravenously at 5 min before [^{11}C]FIMX (204 MBq; 78.6 GBq/ μmol). In each experiment, PET images of brain were acquired with a microPET Focus 220 scanner

(Siemens Medical Solution; Knoxville, TN) for 90 min with scan durations ranging from 30 s to 5 min. The position of the head was fixed using a stereotaxic frame. Electrocardiogram, body temperature, heart, and respiration rates were monitored throughout the experiment.

Image analysis—Images were reconstructed using Fourier rebinning plus two-dimensional filtered back-projection. PET images were co-registered to a standardized monkey MRI template using SPM5 (Wellcome Trust Centre, London, UK). A set of 34 predefined brain regions of interest from the template were then applied to the co-registered PET image to obtain regional decay-corrected time-activity curves. All PET images were corrected for attenuation and scatter. Cerebellar gray matter, which is not included in the template, was delineated semiautomatically using isocontour regions of interest. Uptake of radioactivity in each region of interest was expressed as SUV.

Compartmental modeling—Total distribution volumes (V_T) [46] were estimated for different regions by a two-tissue compartmental model [46] using the PET brain time-activity curves and the measured metabolite-corrected arterial input function. The temporal stabilities of V_T in cerebellum and other regions in the baseline and preblock experiments were assessed by estimating V_T from progressively time-truncated data sets. The PET data analysis was performed using PMOD (PMOD Technologies Ltd.; Zurich, Switzerland).

4 Conclusions

FIMX, labeled in the carbonyl group with carbon-11 as described here, shows excellent imaging characteristics for monkey brain mGluR1 that are clearly superior to those of [^{11}C]ITMM or [^{11}C]ITDM, and highly comparable to those of [^{18}F]FIMX [21]. [^{11}C]FIMX provides an alternative shorter-lived radioligand for studies where it would be efficient to have two radioligand injections into the same subject on the same day, such as in receptor occupancy studies.

Acknowledgments

This work was supported by the Intramural Research Program of the National Institutes of Health (NIMH; ZIA-MH002793). The authors are grateful to the NIH Clinical PET Center (Chief: Dr. P. Herscovitch) for the production of carbon-11.

References

1. Nakanishi S. Molecular diversity of glutamate receptors and implications for brain function. *Science*. 1992; 258:597–603. [PubMed: 1329206]
2. Spooren W, Ballard T, Gasparini F, Amalric M, Mutel V, Schreiber R. Insight into the function of Group I and Group II metabotropic glutamate (mGlu) receptors: behavioural characterization and implications for the treatment of CNS disorders. *Behav Pharmacol*. 2003; 14:257–277. [PubMed: 12838033]
3. Hamill TG, Krause S, Ryan C, Bonnefous C, Govek S, Seiders TJ, et al. Synthesis, characterization, and first successful monkey imaging studies of metabotropic glutamate receptor subtype 5 (mGluR5) PET radiotracers. *Synapse*. 2005; 56:205–216. [PubMed: 15803497]
4. Mutel V, Ellis GJ, Adam G, Chaboz S, Nilly A, Messer J, et al. Characterization of [^3H]quisqualate binding to recombinant rat metabotropic glutamate 1a and 5a receptors and to rat and human brain sections. *J Neurochem*. 2000; 75:2590–2601. [PubMed: 11080213]

5. Fotuhi M, Sharp AH, Glatt CE, Hwang PM, Von Krosigk M, Snyder SH, et al. Differential localization of phosphoinositide-linked metabotropic glutamate receptor (mGluR1) and the inositol 1,4,5-triphosphate receptor in rat brain. *J Neurosci*. 1993; 13:2001–2012. [PubMed: 8386753]
6. Bordi F, Ugolini A. Group 1 metabotropic glutamate receptors: implications for brain diseases. *Prog Neurobiol*. 1999; 59:55–79. [PubMed: 10416961]
7. Ferraguti F, Crepaldi L, Nicoletti F. Metabotropic 1 receptor: current concepts and perspectives. *Pharmacol Rev*. 2008; 60:536–581. [PubMed: 19112153]
8. Kew JNC. Positive and negative allosteric modulation of metabotropic glutamate receptors: emerging therapeutic potential. *Pharmacol Ther*. 2004; 104:233–244. [PubMed: 15556676]
9. Swanson CJ, Bures M, Johnson MP, Linden AM, Monn JA, Schoepp DD. Metabotropic glutamate receptors as novel targets for anxiety and stress disorders. *Nature Rev Drug Discovery*. 2005; 4:131–144. [PubMed: 15665858]
10. Conn PJ. Physiological roles and therapeutic potential of metabotropic glutamate receptors. *Ann N Y Acad Sci*. 2003; 1003:12–21. [PubMed: 14684432]
12. Schkeryantz JM, Kingston AE, Johnson MP. Prospects for metabotropic glutamate 1 receptor antagonists in the treatment of neuropathic pain. *J Med Chem*. 2007; 50:2563–2568. [PubMed: 17489573]
11. Moghaddam B. Targeting metabotropic glutamate receptors for treatment of the cognitive symptoms of schizophrenia. *Psychopharmacol (Berl)*. 2004; 174:39–44.
13. Wu WL, Burnett DA, Domalski M, Greenlee WJ, Li C, Bertorelli R, et al. A Discovery of orally efficacious tetracyclic metabotropic glutamate receptor 1 (mGluR1) antagonists for the treatment of chronic pain. *J Med Chem*. 2007; 50:5550–5553. [PubMed: 17929793]
14. Mu LJ, Schubiger PA, Ametamey SM. Radioligands for the PET imaging of metabotropic glutamate receptor subtype 5 (mGluR5). *Curr Topics Med Chem*. 2010; 10:1558–1568.
15. Brown AK, Kimura Y, Zoghbi SS, Siméon FG, Liow JS, Kreisl WC, et al. Metabotropic glutamate subtype 5 receptors are quantified in the human brain with a novel radioligand for PET. *J Nucl Med*. 2008; 49:2042–2048. [PubMed: 19038998]
16. Wong DF, Waterhouse R, Kuwabara H, Kim J, Brasic JR, Chamroonrat W, et al. F-18-FPEB, a PET radiopharmaceutical for quantifying metabotropic glutamate 5 receptors: a first-in-human study of radiochemical safety, biokinetics, and radiation dosimetry. *J Nucl Med*. 2013; 54:388–396. [PubMed: 23404089]
17. Hostetler ED, Eng W, Joshi AD, Sanabria-Bohórquez S, Kawamoto H, Ito S, et al. Synthesis, characterization, and monkey PET studies of [¹⁸F]MK-1312, a PET tracer for quantification of mGluR1 receptor occupancy by MK-5435. *Synapse*. 2011; 65:125–135. [PubMed: 20524178]
18. Yamasaki T, Fujinaga M, Maeda J, Kawamura K, Yui J, Hatori A, et al. Imaging for metabotropic glutamate receptor subtype 1 in rat and monkey brains using PET with [¹⁸F]FITM. *Eur J Nucl Med Mol Imaging*. 2012; 39:632–641. [PubMed: 22113620]
19. Fujinaga M, Yamasaki T, Maeda J, Yui J, Nagai Y, Nengaki N, et al. Development of *N*-[4-isopropylamino]pyrimidin-4-yl]-1,3-thiazol-2-yl]-*N*-methyl-4-[¹¹C]methylbenzamide for positron emission tomography imaging of metabotropic glutamate 1 receptor in monkey brain. *J Med Chem*. 2012; 55:11042–11051. [PubMed: 23194448]
20. Zanotti-Fregonara P, Barth VN, Liow J-S, Zoghbi SS, Clark DT, Rhoads E, et al. Evaluation in vitro and in animals of a new ¹¹C-labeled PET radioligand for metabotropic glutamate receptors 1 in brain. *Eur J Nucl Med Mol Imaging*. 2013; 40:245–253. [PubMed: 23135321]
21. Xu R, Zanotti-Fregonara P, Zoghbi SS, Gladding RL, Woock AE, Innis RB, et al. Synthesis and evaluation in monkey of [¹⁸F]4-fluoro-*N*-methyl-*N*-(4-(6-(methylamino)pyrimidin-4-yl)thiazol-2-yl)benzamide ([¹⁸F]FIMX): a promising radioligand for PET imaging of brain metabotropic glutamate receptor1 (mGluR1). *J Med Chem*. 2013; 56:9146–9155. [PubMed: 24147864]
22. Li S, Huang Y. *In vivo* imaging of the metabotropic glutamate receptor 1 (mGluR1) with positron emission tomography: recent advances and perspective. *Curr Med Chem*. 2014; 21:113–123. [PubMed: 23992339]
23. Yamasaki T, Maeda J, Fujinaga M, Nagai Y, Hatori A, Yui J, et al. PET brain kinetics of ¹¹C-ITMM and ¹¹C-ITDM radioprobes for metabotropic glutamate receptor type 1, in a nonhuman primate. *Am J Nucl Med Mol Imaging*. 2014; 4:260–269. [PubMed: 24795840]

24. Toyohara J, Sakata M, Oda K, Ishii K, Ito K, Hiura M, et al. Initial human PET studies of metabotropic glutamate receptor type 1 ligand C-11-ITMM. *J Nucl Med*. 2013; 54:1302–1307. [PubMed: 23804329]
25. Zanotti-Fregonara P, Xu R, Zoghbi SS, Liow J-S, Fujita M, Veronese M, et al. The positron emission tomographic radioligand ¹⁸F-FIMX images and quantifies metabotropic glutamate receptor 1 in proportion to the regional density of its gene transcript in human brain. Submitted.
26. Hjorth, S.; Karlsson, C.; Jucaite, A.; Varnäs, K.; Wählby Hamrén, U.; Johnström, P., et al. A PET study comparing receptor occupancy by five selective cannabinoid 1 receptor antagonists in non-human primates. *Neuropharmacology*. <http://dx.doi.org/10.1016/j.neuropharm.2015.03.002>
27. Pike VW. PET Radiotracers: crossing the blood-brain barrier and surviving metabolism. *Trends Pharmacol Sci*. 2009; 30:431–440. [PubMed: 19616318]
28. Zeisler SK, Nader M, Theobald A, Oberdorfer F. Conversion of no-carrier-added [¹¹C]carbon dioxide to [¹¹C]carbon monoxide on molybdenum for the synthesis of ¹¹C-labelled aromatic ketones. *Appl Radiat Isot*. 1997; 48:1091–1095.
29. Långström B, Itsenko O, Rahman O. [¹¹C]Carbon monoxide, a versatile and useful precursor in labelling chemistry for PET-ligand development. *J Labelled Compd Radiopharm*. 2007; 50:794–810.
30. Kihlberg T, Långström B. Biologically active ¹¹C-labeled amides using palladium-mediated reactions with aryl halides and [¹¹C]carbon monoxide. *J Org Chem*. 1999; 64:9201–9205.
31. Donohue SR, Halldin C, Schou M, Hong J, Phebus L, Chernet E, et al. Radiolabeling of a high potency cannabinoid subtype-1 receptor ligand, *N*-(4-fluoro-benzyl)-4-(3-(piperidin-1-yl)-indole-1-sulfonyl)benzamide (PipISB), with carbon-11 or fluorine-18. *J Labelled Compd Radiopharm*. 2008; 51:146–152.
32. Dahl K, Schou M, Amini N, Halldin C. Palladium-mediated [¹¹C]carbonylation at atmospheric pressure: a general method using Xantphos as supporting ligand. *Eur J Org Chem*. 2013:1228–1231.
33. Andersen TL, Friis SD, Audrain H, Nordeman P, Antoni G, Skrydstrup T. Efficient C-11-carbonylation of isolated aryl palladium complexes for PET: application to challenging radiopharmaceutical synthesis. *J Am Chem Soc*. 2015; 137:1548–1555. [PubMed: 25569730]
34. Smith, D. Synthia gets extreme makeover courtesy of National Instruments. 2008. p. 24-25. <ftp://ftp.ni.com/pub/branches/.../NIDaysBooklet.pdf>
35. Bjurling, P.; Reineck, R.; Westerburg, G.; Gee, AD.; Sutcliffe, J.; Långström, B. Synthia, a compact radiochemistry system for automated production of radiopharmaceuticals. In: Link, JM.; Ruth, TJ., editors. *Proceedings Sixth Workshop on Targetry and Target Chemistry, TRIUMF, Vancouver*. 1995. p. 282-284.
36. Kihlberg T, Långström B. Method and apparatus for production of [¹¹C]carbon monoxide in labeling synthesis. *PCT Int Appl*. 2002 WO2002/102711.
37. Pike VW. Positron-emitting radioligands for studies in vivo probes for human psychopharmacology. *J Psychopharmacol*. 1993; 7:139–158. [PubMed: 22290661]
38. Waterhouse RN. Determination of lipophilicity and its use as a predictor of blood-brain barrier penetration of molecular imaging agents. *Mol Imaging Biol*. 2003; 5:376–389. [PubMed: 14667492]
39. Laruelle M, Slifstein M, Huang Y. Relationships between radiotracer properties and image quality in molecular imaging of the brain with positron emission tomography. *Mol Imaging Biol*. 2003; 5:363–375. [PubMed: 14667491]
40. Patel S, Gibson R. In vivo site-directed radiotracers: a minireview. *Nucl Med Biol*. 2008; 35:805–815. [PubMed: 19026942]
41. Zoghbi SS, Anderson KB, Jenko KJ, Luckenbaugh DA, Innis RB, Pike VW. On quantitative relationships between drug-like compound lipophilicity and plasma free fraction in monkey and human. *J Pharm Sci*. 2012; 101:1028–1039. [PubMed: 22170327]
42. Lavreysen H, Wouters R, Bischoff F, Pereira SN, Langlois X, et al. JNJ16259685, a highly potent, selective and systemically active mGlu1 receptor antagonist. *Neuropharmacology*. 2004; 47:961–972. [PubMed: 15555631]

43. Zoghbi SS, Shetty HU, Ichise M, Fujita M, Imaizumi M, Liow JS, et al. PET imaging of the dopamine transporter with ^{18}F -FECNT: a polar radiometabolite confounds brain radioligand measurements. *J Nucl Med.* 2006; 47:520–527. [PubMed: 16513622]
44. Gandelman MS, Baldwin RM, Zoghbi SS, Zea-Ponce Y, Innis RB. Evaluation of ultrafiltration for the free-fraction determination of single photon emission computed tomography (SPECT) radiotracers: β -CIT, IBF, and iomazenil. *J Pharm Sci.* 1994; 83:1014–1019. [PubMed: 7965658]
45. Clark, JD.; Baldwin, RL.; Bayne, KA.; Brown, MJ.; Gebhart, GF.; Gonder, JC., et al. *Guide for the Care and Use of Laboratory Animals.* 8. National Academy Press; 1996.
46. Innis RB, Cunningham VJ, Delforge J, Fujita M, Gjedde A, Gunn RN, et al. Consensus nomenclature for in vivo imaging of reversibly binding radioligands. *J Cerebr Blood Flow Metab.* 2007; 27:1533–1539.

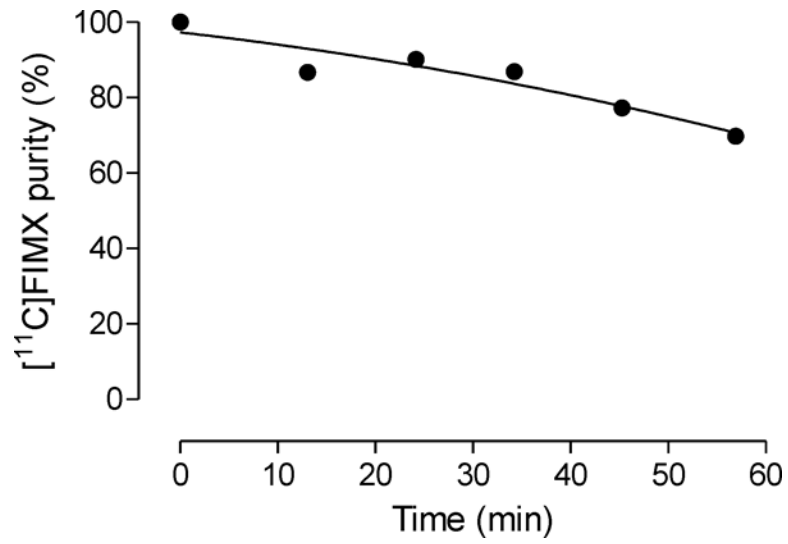


Fig. 1. Decline in [¹¹C]FIMX radiochemical purity in sodium phosphate buffer (0.15 M, pH 7.4) at room temperature.

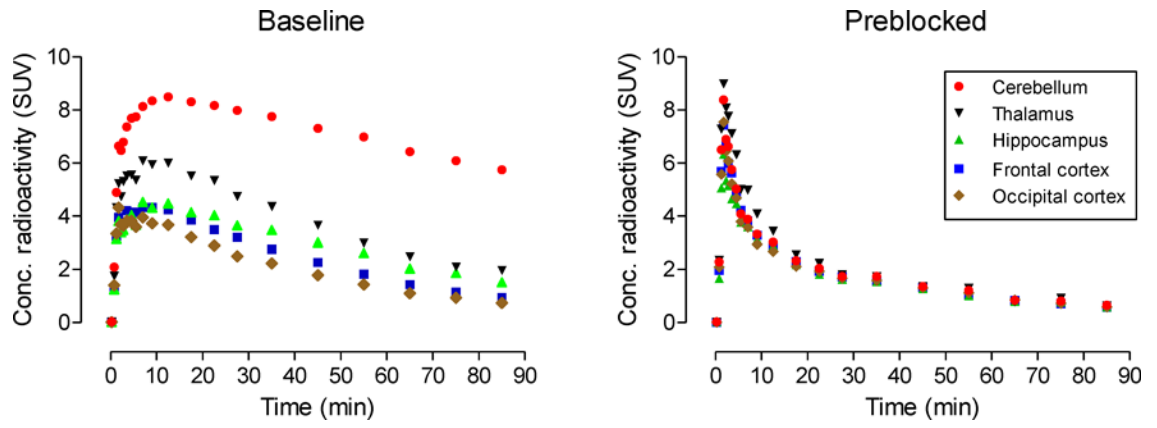


Fig. 2. PET time-activity curves in selected brain regions of a rhesus monkey administered [¹¹C]FIMX at baseline (left panel), and after preblock of mGluR1 with the selective antagonist JNJ16259685 (3 mg/kg, i.v.) (right panel).

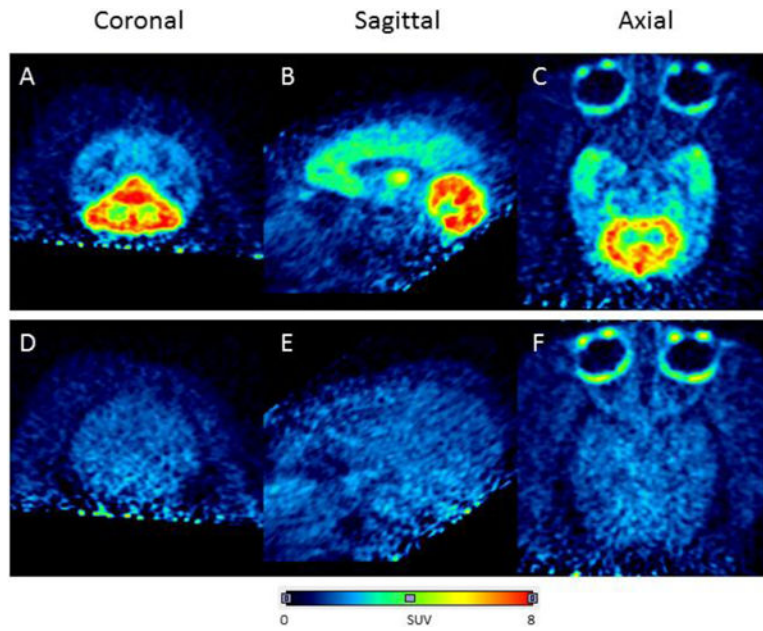


Fig. 3. Brain PET images acquired as summed data from 0–90 min after intravenous injection of anesthetized rhesus monkey with [^{11}C]FIMX (~ 200 MBq) at baseline (top row) and after preblock of mGluR1 with the selective antagonist JNJ16259685 (3 mg/kg, i.v.) (bottom row). Panels A and D are coronal, B and E, sagittal, and C and F transaxial images, respectively.

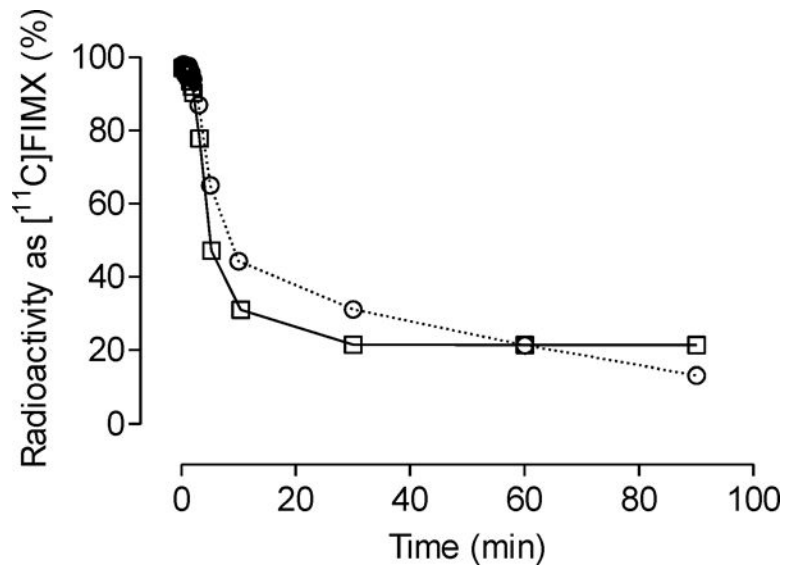


Fig. 4. Time course of the percentage of plasma radioactivity represented by unchanged $[^{11}\text{C}]$ FIMX after intravenous injection into monkey under baseline (\square) and prebloc (\circ) conditions.

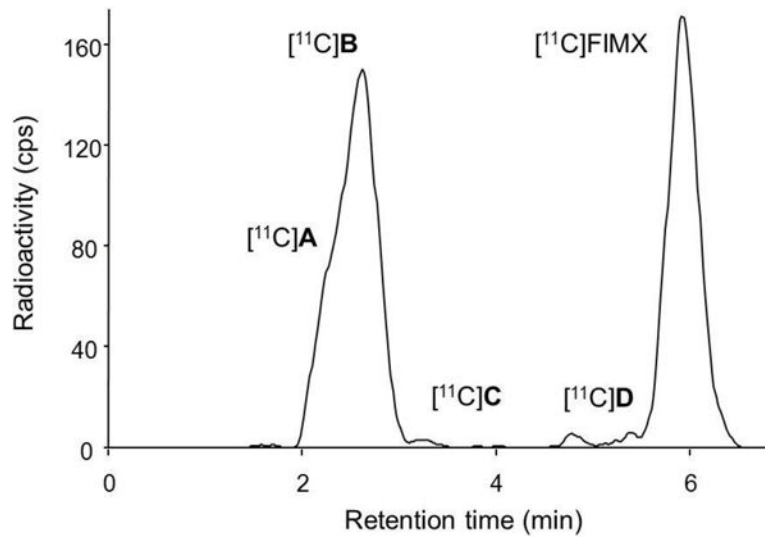


Fig. 5. Radiochromatogram from the HPLC analysis of monkey plasma at 30 min after intravenous injection of [^{11}C]FIMX at baseline.

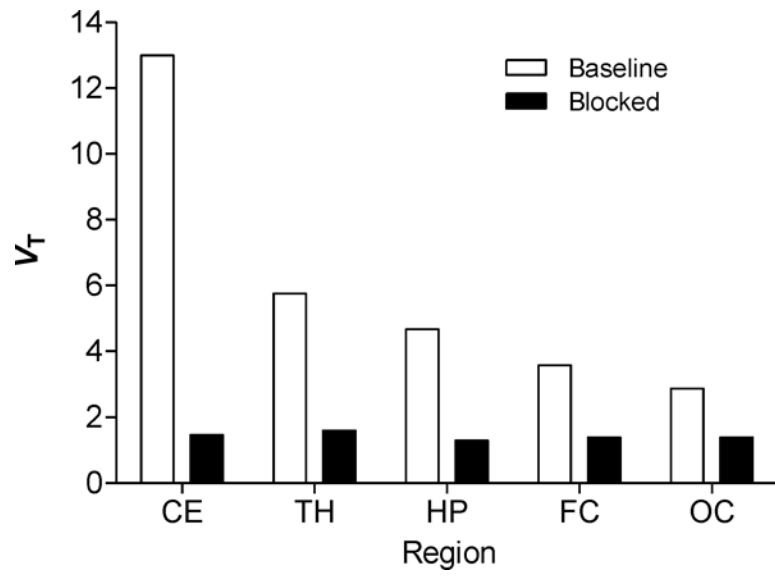


Fig. 6. $[^{11}\text{C}]$ FIMX distribution volume (V_T) values under baseline and preblocked conditions calculated for selected brain regions using a two-tissue compartmental model. Brain regions: CE, cerebellum; TH, thalamus; HP, hippocampus; FC, frontal cortex; OC, occipital cortex.

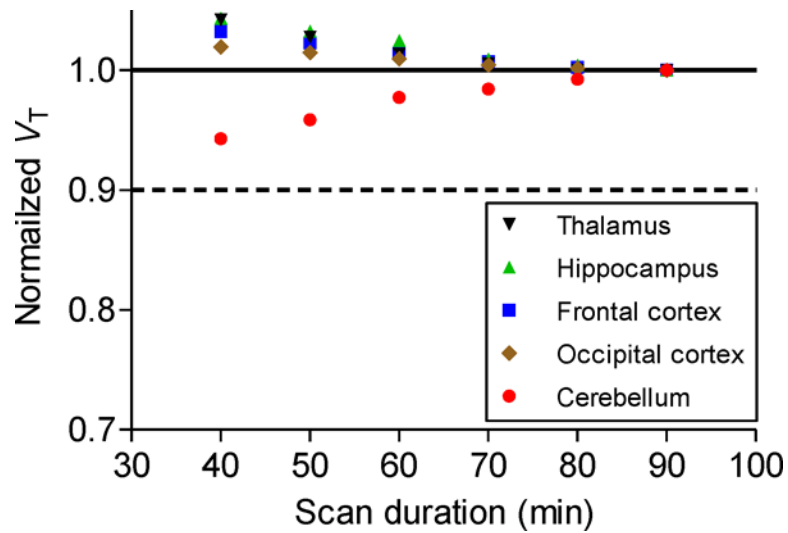
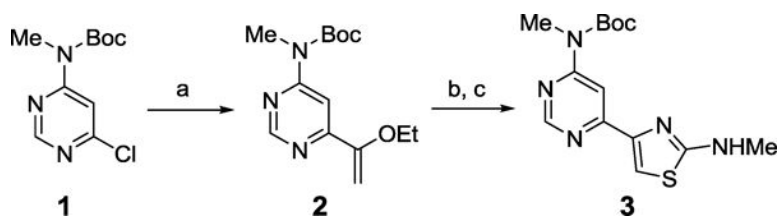
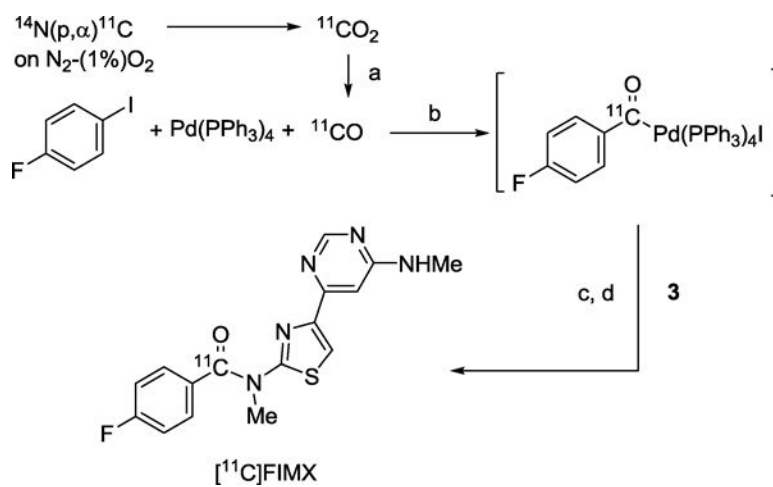


Fig. 7. Normalized distribution volume (V_T) as a function of duration of image acquisition after [^{11}C]FIMX injection at baseline in rhesus monkey. V_T was calculated for selected brain regions using a two-tissue compartmental model and normalized to a fraction of the V_T value from 90-min data.

**Scheme 1.**

Synthesis of Boc-protected amine precursor (**3**). Conditions and yields: (a) *tri*-butyl(1-ethoxyvinyl)stannane, Pd(PPh₃)₄, CsF, CuI, DMF, 80 °C, 5.5 h; 66%. (b) NBS, THF/H₂O, rt, 2 h; (c) 1-methyl thiourea, rt, 2 h; 94% (for b and c together).

**Scheme 2.**

Synthesis of $[^{11}\text{C}]$ FIMX via Pd-mediated ^{11}C -carbonylation of 1-fluoro-4-iodobenzene followed by aminolysis of $[^{11}\text{C}]$ acylpalladium complex, and Boc deprotection. Conditions: (a) Mo, 875 °C; (b) THF, 130 °C, 4 min; (c) Bu_3N , 80–110 °C, 6 min, evaporate to dryness; (d) HCl in THF, 100 °C, 1 min.

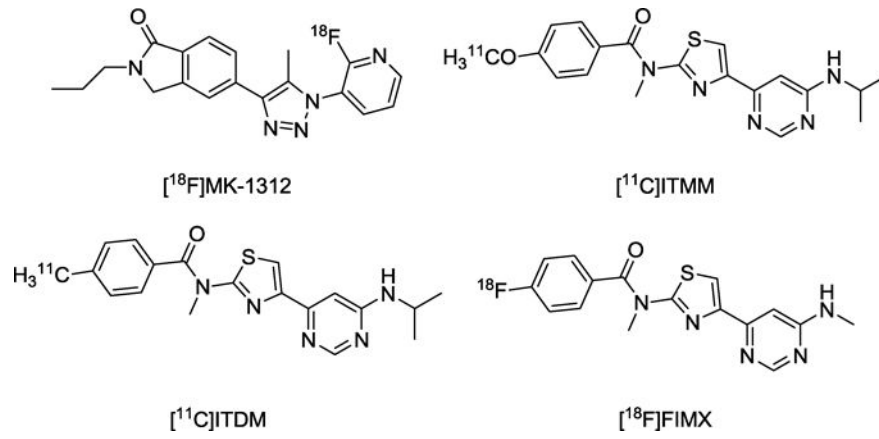


Chart 1.
Prominent PET radioligands for imaging mGluR1.